



# International Journal of Innovative Research in Science Engineering and Technology (IJIRSET)

*(A Monthly, Peer Reviewed, Refereed, Scholarly Indexed, Open Access Journal)*



**Impact Factor: 8.699**

**Volume 14, Issue 4, April 2025**

# **Design and Analysis of mmWave Patch Antenna for 5G And 6G Applications**

**S. Mohan Rao, Bolleddula Bhavani Shankar, Thotli Pavithra, Kambam Rajesh Reddy,  
Rayapu Vamsi, Sudha Sreenadha**

Assistant Professor, Department of ECE, Sri Venkateswara College of Engineering, Tirupati, AP, India

UG Scholars, Department of ECE, Sri Venkateswara College of Engineering, Tirupati, AP, India

**ABSTRACT:** This paper presents the design, simulation, and analysis of a compact millimeter-wave (mmWave) patch antenna optimized for multi-band operation targeting 5G and emerging 6G communication systems. The proposed antenna operates efficiently at 24.5 GHz, 26.63 GHz, 29.375 GHz, and 31.35 GHz, offering high gain, low sidelobe levels, and effective impedance matching. The antenna structure integrates a circular patch with an embedded slotted H-shaped element, enhancing multi-resonant behavior while maintaining a compact form factor. Precise geometrical tuning of the slots, feedline, and parasitic elements enables multi-band resonance and directional radiation characteristics. Simulations were conducted using CST Studio Suite®, analyzing S-parameters, VSWR, and radiation patterns. The antenna exhibits return loss values below  $-10$  dB across all operational bands and achieves a peak gain of 6.38 dBi at 31.35 GHz. The corresponding VSWR remains under 1.5 at key frequencies, indicating efficient power transfer. Far-field analysis reveals focused radiation patterns with low sidelobe levels, suitable for high-frequency beam-steering applications. Additionally, 3D gain plots demonstrate directional behavior with minimal losses, confirmed by high radiation and total efficiency values.

The design's performance suggests strong potential for deployment in advanced mmWave systems, including 5G/6G base stations, satellite links, and precision-guided communication systems.

**KEYWORDS :** 5G, 6G, mm wave Antenna, CST Studio, Millimeter-wave, High Efficiency etc.

## **I. INTRODUCTION**

The exponential growth in mobile data traffic and the proliferation of smart devices have driven the demand for next-generation wireless communication systems, particularly fifth-generation (5G) and emerging sixth-generation (6G) networks. These systems aim to provide ultra-high-speed connectivity, low latency, and massive device connectivity. To meet these requirements, millimeter-wave (mmWave) frequency bands, typically ranging from 24 GHz to 100 GHz, have been proposed as a viable solution due to the large bandwidth availability [11], [12].

The antenna, as a critical component in any wireless system, plays a pivotal role in determining the overall system performance. However, designing antennas for mmWave bands poses significant challenges due to the trade-offs between gain, size, isolation, bandwidth, and efficiency. In this context, Multiple-Input Multiple-Output (MIMO) technology has emerged as a key enabler, offering increased capacity and link reliability. MIMO antennas for mmWave 5G applications require compact form factors, wide impedance bandwidth, low mutual coupling, and high gain to counter the high propagation loss associated with mmWave frequencies [4], [5], [6].

Various researchers have investigated compact and high-gain antenna designs suitable for integration in mobile and wearable devices. For instance, Lin et al. [3] developed a circularly polarized antenna at 28 GHz, while Iqbal et al. [2] presented an EBG-backed antenna system for wearable applications. The use of dielectric resonators [7], slot-fed structures [4], and substrate integrated waveguides (SIW) [5] has also shown promise in improving bandwidth and isolation performance. Additionally, metamaterial structures have gained considerable attention for their ability to enhance antenna gain and reduce size [1], [10], [15].

Despite significant progress, several challenges persist in the design of mmWave MIMO antennas for 5G/6G applications:

- *High Mutual Coupling:* MIMO configurations often suffer from mutual coupling between antenna elements, degrading system performance [6], [8].
- *Limited Bandwidth and Gain:* Achieving wideband operation with high gain in a compact design is complex due to space constraints and material limitations [9], [16], [17].
- *Polarization Diversity:* Many designs lack efficient polarization diversity, which is essential for improving signal reception and reducing multipath fading [4].
- *Integration with Smart Devices:* Ensuring seamless integration in small-form-factor devices without compromising performance remains a key issue [7], [8].
- *Lack of AI/ML Optimization:* While some works have explored AI-driven antenna optimization [14], its application in mmWave antenna design is still limited.

Given these challenges, there is a pressing need to design a compact, high-isolation, wideband MIMO antenna that is suitable for 5G mmWave applications. Additionally, leveraging novel geometries, such as metamaterial-inspired structures and decoupling elements, can lead to performance enhancements in terms of gain, bandwidth, and isolation. These advancements will facilitate the integration of such antennas into smart mobile terminals, wearable devices, and IoT modules.

The primary objectives of this paper are:

1. To design a compact  $2 \times 2$  MIMO antenna operating in the mmWave band, specifically around 28 GHz.
2. To achieve high isolation between the antenna elements using integrated decoupling structures.
3. To enhance gain and bandwidth using metamaterial-inspired or branched-slot geometries.
4. To analyze key performance parameters including S-parameters, envelope correlation coefficient (ECC), diversity gain, and far-field radiation patterns.

The major contributions of this work are summarized as follows:

- A novel  $2 \times 2$  compact MIMO antenna is proposed for mmWave 5G/6G applications using CST Studio Suite.
- The antenna incorporates decoupling structures to improve isolation without increasing footprint.
- Metamaterial-inspired designs are utilized to enhance gain and bandwidth in a compact layout.
- Detailed performance evaluation is conducted using simulation, focusing on key parameters relevant for MIMO performance.
- The proposed design is benchmarked against recent state-of-the-art works to demonstrate its efficacy.

The remainder of the paper is structured as follows: section II provides the literature survey and Section III provides a detailed overview of the antenna design methodology and materials used. Section IV presents the simulation setup and discusses the results, including S-parameters, ECC, gain, and radiation patterns. Section V concludes the paper and suggests future directions for further research.

## II. LITERATURE SURVEY

The rapid evolution of wireless communication demands high-performance antenna systems, particularly in the millimeter-wave (mmWave) spectrum for 5G and emerging 6G applications. Researchers have proposed various antenna designs and technologies to meet the stringent requirements of bandwidth, gain, compactness, and MIMO compatibility.

Ren et al. [1] explored the use of MEMS technologies for optical metamaterials, highlighting their applicability in high-frequency devices, which can inspire metamaterial-based enhancements in antenna performance. Iqbal et al. [2] proposed a millimeter-wave MIMO antenna with an Electromagnetic Bandgap (EBG) structure for wearable applications, achieving enhanced isolation and reduced mutual coupling. Similarly, Lin et al. [3] designed a compact omnidirectional circularly polarized antenna at 28 GHz for device-to-device communication in 5G systems, emphasizing the significance of polarization diversity.

Ullah et al. [4] introduced a series-slot-fed circularly polarized MIMO array for indoor 5G applications, enhancing polarization and spatial diversity. Usman et al. [5][6] developed a dual-port annular slot MIMO antenna and a dielectric

resonator-based design with improved isolation, both operating in the mmWave bands. Sharawi et al. [7] proposed a dielectric resonator-based MIMO system suitable for mobile mmWave devices, focusing on integration and miniaturization.

Alhaqbani et al. [8] and Bait-Suwailam et al. [9] designed wideband MIMO antennas with hexagonal slots and compact decoupling structures respectively, aiming to enhance bandwidth and reduce mutual coupling for 5G terminals. Liu et al. [10] reported gain enhancement in microstrip antennas using negative permeability meta materials, reinforcing the role of engineered materials in antenna improvement.

The fundamental role of mmWave in future broadband systems was emphasized by Pi and Khan [11], while Xu et al. [12] presented various mmWave antenna designs tailored for 5G applications. Park and Lee [13] reviewed beamforming techniques in mmWave antennas, essential for overcoming propagation challenges in 5G.

Yadav et al. [14] explored AI-based optimization methods for 5G antenna performance, marking a shift toward intelligent design. Zhang and Huang [15] discussed metamaterial-inspired antennas that enhance performance without increasing size. Lee et al. [16] presented a high-gain antenna for small-cell deployments in 5G, a key to dense urban network layouts. Wang et al. [17] designed a novel mmWave MIMO antenna with superior gain and isolation. Most recently, Talari and Sekhar [18] introduced a high-gain dual-band metamaterial-inspired antenna with a hexagonal structure, demonstrating its effectiveness in 5G spectrum bands.

This body of literature highlights the advancements and challenges in mmWave antenna design. Common themes include gain enhancement, miniaturization, MIMO integration, and the application of metamaterials and AI in design optimization. These works form the foundation for further innovation in antenna structures targeting future 6G communication standards.

### III. DESIGN METHODOLOGY

The proposed antenna design introduces a novel structure aimed at achieving high gain, compactness, and multi-band performance for millimeter-wave (mmWave) applications, particularly around the 28 GHz frequency band. The antenna geometry integrates a circular radiating patch with a slotted H-shaped structure embedded within it, coupled with a microstrip feedline and strategically engineered ground plane features.

#### A. Antenna Configuration

At the heart of the design is a circular patch radiator, selected for its inherent wideband behavior and efficient radiation characteristics. This patch has a diameter that supports resonance within the mmWave spectrum and serves as the primary radiating element. Embedded inside this circular patch is a slotted H-shaped structure, whose geometry has been meticulously optimized to support multiple resonant frequencies.

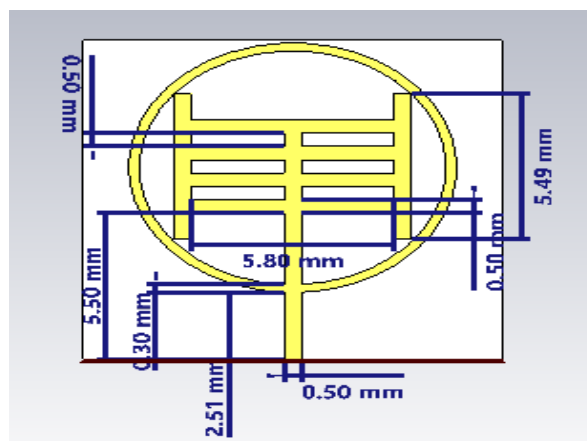


Fig. 1. Antenna Design

The H-shaped slot, functioning as a parasitic element, introduces additional current paths and modifies the surface current distribution. This generates multiple resonant modes and significantly enhances bandwidth and radiation efficiency. The vertical bars of the H-structure are 5.49 mm in length, while the horizontal bar sits 5.50 mm from the substrate's top and spans 5.8 mm in length. Slot width is maintained at 0.5 mm for effective frequency tuning.

#### *B. Feeding Mechanism and Ground Structure*

The antenna is excited through a microstrip feedline, which is 0.5 mm wide and extends 5.5 mm toward the patch. A gap of 0.3 mm is maintained between the feedline and the lower bar of the H-shaped slot to facilitate proper impedance matching and efficient power coupling. This gap is crucial for controlling the input reflection coefficient and minimizing return loss. The ground plane is partially slotted to refine the current path and enhance radiation properties. It features a rectangular slot (3 mm × 2.6 mm) and a circular slot with a radius of 0.4 mm, both contributing to bandwidth improvement and resonant frequency control.

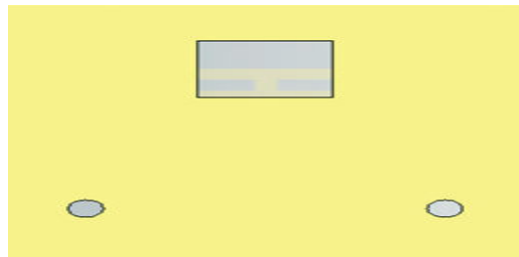


Fig. 2. Ground Structure

#### *C. Substrate and Dielectric Considerations*

The structure is built on a low-loss dielectric substrate with a thickness of 0.203 mm, ideal for high-frequency mmWave performance. A thinner substrate helps in reducing surface wave losses and enhancing the antenna gain, while maintaining a compact form factor suitable for modern wireless devices.



Fig. 3. Substrate

#### *D. Metamaterial-Inspired Ring*

To further enhance the performance, a ring-shaped structure is embedded concentrically within the patch. This ring has an inner radius of 4.4 mm and an outer radius of 4.7 mm, giving a ring width of 0.3 mm. Acting similarly to metamaterial-inspired resonators, this ring improves radiation pattern stability and contributes to gain enhancement by introducing additional coupling effects.

#### *E. Geometrical Summary*

All relevant design dimensions are summarized in Table I, ensuring reproducibility and clarity in fabrication.

TABLE I. ANTENNA GEOMETRY PARAMETERS

Parameter	Value (mm)
Patch Width	12
Patch Length	12
Ground Slot Width	3
Ground Slot Length	2.6
Ground Circle Slot Radius	0.4
Substrate Thickness	0.203
Feed Width	0.5
Feed Length (up to rectangular bar)	5.5
Horizontal Rectangular Bar Length	5.8
Bar Width	0.5
Gap Width	0.3
Vertical Bar Length	5.49
Ring Width	0.3
Ring Inner Radius	4.4
Ring Outer Radius	4.7

F. Design Goals

The design aims to fulfill the following objectives:

- Achieve multi-band operation suitable for mmWave communication systems.
- Maintain compact size for integration into portable wireless terminals.
- Provide enhanced gain and radiation efficiency through geometric and parasitic optimization.
- Ensure good impedance matching with low reflection coefficients across operating bands

IV. SIMULATION RESULTS

The graph illustrates the S11 (return loss) of the proposed antenna from 20 GHz to 32 GHz, showing multiple resonant frequencies with return loss values below -10 dB, indicating good impedance matching. Notable deep dips occur at 24.51 GHz (-17.10 dB), 29.38 GHz (-26.50 dB), and 31.35 GHz (-29.07 dB), reflecting excellent radiation efficiency at these frequencies. Other points near -10 dB (24.34 GHz, 24.66 GHz, 29.31 GHz, 29.46 GHz, 31.19 GHz, and 31.48 GHz) confirm acceptable matching across a wide band. These results highlight the antenna’s capability to operate efficiently across multiple mmWave bands, making it suitable for 5G and future 6G applications.

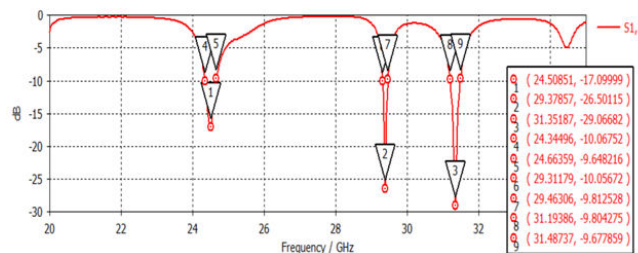


Fig. 4. S parameter waveform

The graph shows the Voltage Standing Wave Ratio (VSWR) of the proposed antenna from 20 GHz to 35 GHz, highlighting its impedance matching performance. Ideal VSWR is 1:1, with values below 1.5 indicating efficient power transfer. The antenna demonstrates excellent matching at 29.375 GHz (VSWR 1.09) and 31.365 GHz (VSWR 1.13), and good matching at 24.48 GHz (VSWR 1.31). However, a high VSWR of 3.61 at 34.45 GHz indicates poor matching and inefficiency at that frequency, which lies outside the antenna’s intended operational band. Overall, the low VSWR values across key mmWave frequencies confirm the antenna's suitability for 5G and future 6G applications.

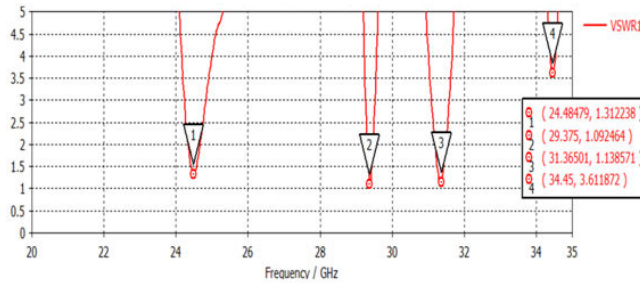


Fig. 5. VSWR waveform

This image shows the far-field radiation patterns of the proposed antenna at 24.5 GHz, 29.375 GHz, and 31.35 GHz, plotted in polar form with Phi fixed at 90°. At 24.5 GHz, the pattern is moderately directional with a main lobe centered around 0°, indicating effective radiation. At 29.375 GHz, the pattern becomes more focused with a sharper main lobe and reduced sidelobes, reflecting better directivity and higher gain. The 31.35 GHz pattern maintains this directionality and efficiency, showing consistent performance. Overall, the antenna demonstrates strong, directional radiation across all target frequencies, supporting its suitability for multi-band mmWave applications in 5G and 6G systems.

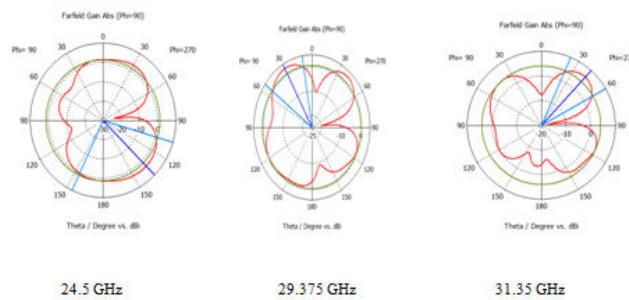


Fig. 6. Farfield radiation pattern at 29.375 GHz, 31.35 GHz

This image displays the far-field radiation patterns of the proposed antenna at 29.375 GHz, 31.35 GHz, and 24.5 GHz in polar plots, showing gain (in dBi) versus Phi angle with Theta fixed at 90°. These plots reveal the antenna's directional behavior in the horizontal plane. At 29.375 GHz, the pattern exhibits a strong directional lobe centered at 90°, indicating efficient radiation. Similarly, at 31.35 GHz, the antenna maintains a focused main lobe with low sidelobes, showing consistent and effective performance. The 24.5 GHz pattern, while still directional, features a broader beamwidth and slightly different shape, reflecting variation in gain and coverage. Overall, the antenna demonstrates robust directional radiation across the target frequencies, supporting multi-band operation in the mmWave spectrum. The sharp main lobes and low sidelobe levels make it well-suited for 5G and future 6G communication systems. The observed differences across frequencies emphasize the importance of full-band analysis for optimal antenna design.

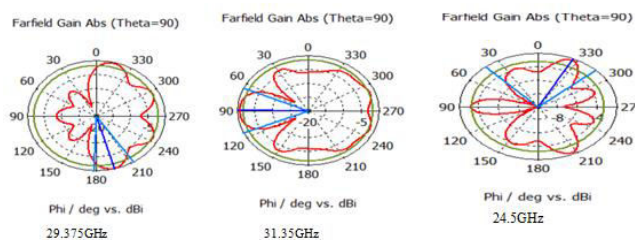


Fig. 7. Farfield radiation pattern at 29.375 GHz, 31.35 GHz

This image displays the 3D far-field radiation pattern of the proposed antenna at 31.35 GHz, highlighting its gain distribution in dBi across space. The pattern features a strong directional main lobe along the positive y-axis, indicating focused radiation in that direction. A color gradient from red (high gain) to dark blue (low gain) illustrates the gain variation, with a peak gain of 6.36 dBi. Low sidelobe levels suggest minimal interference from other directions. The accompanying data shows a radiation efficiency of -1.930 dB and total efficiency of -1.934 dB, indicating low internal losses. Overall, the plot confirms the antenna's effective directional performance at 31.35 GHz, making it suitable for mmWave applications.

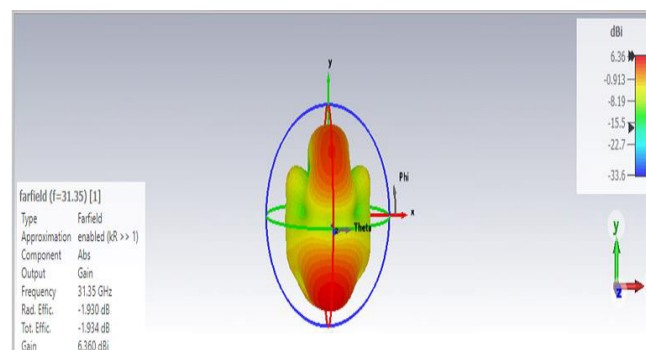


Fig. 8. 3 D Farfield radiation pattern at 31.35 GHz

This image illustrates the 3D far-field radiation pattern of the antenna at 29.375 GHz, showing its gain distribution in dBi across three-dimensional space. The pattern features a directional main lobe pointing along the positive y-axis, indicating focused signal transmission. A color gradient from red (highest gain) to dark blue (lowest gain) visualizes the gain variation, with a peak gain of 3.11 dBi. Low sidelobe levels suggest minimal interference from other directions. The data indicates a radiation efficiency of -2.141 dB and total efficiency of -2.149 dB, reflecting minimal internal losses. Overall, this 3D plot confirms the antenna's effic

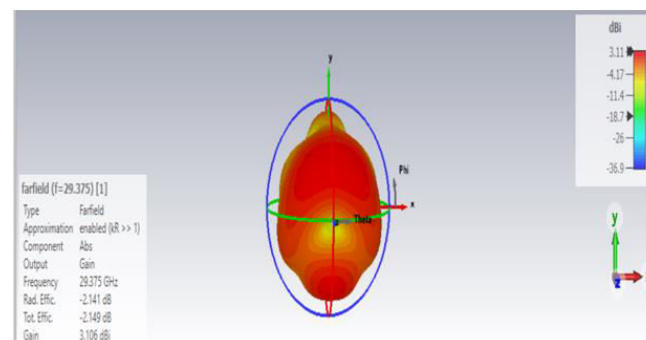


Fig. 9. 3 D Farfield radiation pattern at 29.375 GHz

This image displays the 3D far-field radiation pattern of the antenna at 24.5 GHz, showing its gain distribution in dBi across three-dimensional space. The pattern exhibits a directional main lobe along the positive y-axis, indicating focused radiation. A color gradient from red (highest gain) to dark blue (lowest gain) visualizes gain variation, with a peak gain of 3.57 dBi. The presence of minimal sidelobes suggests reduced interference from other directions. The accompanying data confirms a radiation efficiency of -0.9999 dB and a total efficiency of -1.079 dB, indicating low internal losses. Overall, the plot highlights the antenna's effective directional performance at 24.5 GHz, suitable for mmWave applications.

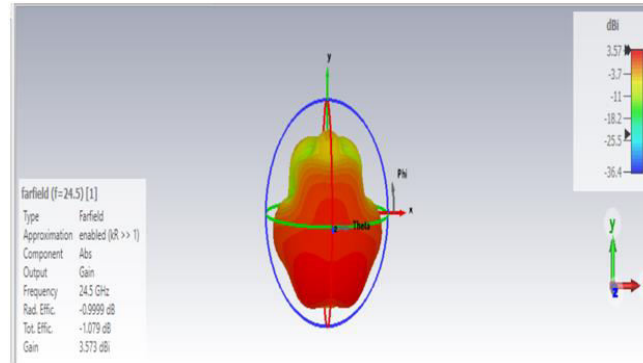


Fig. 10. 3D Farfield radiation pattern at 24.5 GHz

This image illustrates the surface current distribution of the proposed antenna at 24.5 GHz, highlighting the intensity and direction of current flow across the structure. The color gradient—from dark blue (low current) to red (high current)—shows that the peak surface current reaches 1056.56 A/m. The strongest current concentrations appear around the circular patch and H-shaped structure, indicating these areas as the primary radiators. Directional arrows depict the current flow, offering insight into the antenna's resonant behavior. The red line at the base represents the feed line, serving as the main current source. Overall, the image provides a clear understanding of how current distribution influences the antenna's radiation at 24.5 GHz.

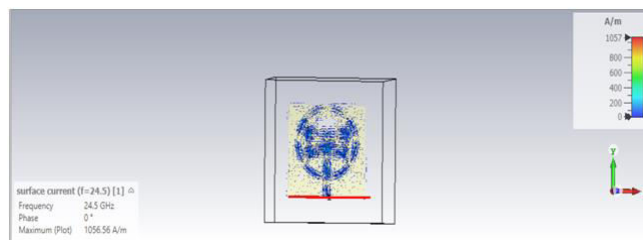


Fig. 11. Surface current distribution at 24.5 GHz

This image displays the surface current distribution of the proposed antenna at 29.375 GHz, highlighting the magnitude and direction of current flow. The color scale—from dark blue (low) to red (high)—shows a peak current of 1162.27 A/m. Current is primarily concentrated around the circular patch and H-shaped structure, indicating their key role in radiation at this frequency. Directional arrows reveal the flow pattern, offering insight into the antenna's resonant behavior. The red line at the base represents the feed line, serving as the main current source. Compared to the 24.5 GHz case, this distribution shows a higher peak current, suggesting stronger excitation at 29.375 GHz. This analysis provides valuable insight into the antenna's efficient performance at this frequency.

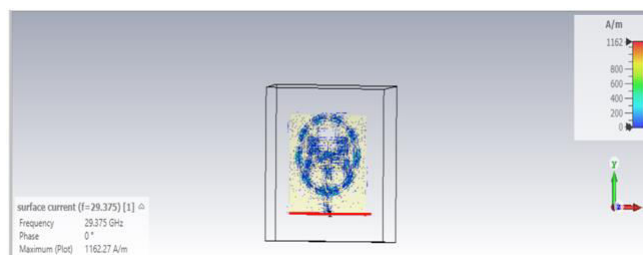


Fig. 12. Surface current distribution at 29.375 GHz

This image illustrates the surface current distribution of the proposed antenna at 31.35 GHz, showing both the magnitude and direction of current flow. The color gradient—from dark blue (low) to red (high)—indicates a peak

current of 760.054 A/m. The strongest current concentrations are observed around the circular patch and H-shaped structure, confirming their role as the primary radiating elements. Directional arrows highlight the current flow path, offering insight into resonant behavior. The red line at the bottom represents the feed line, acting as the main source of excitation. Compared to the distributions at 24.5 GHz and 29.375 GHz, this frequency exhibits a lower peak current, suggesting a variation in excitation strength. Overall, the image provides a clear understanding of the antenna's radiation behavior at 31.35 GHz.

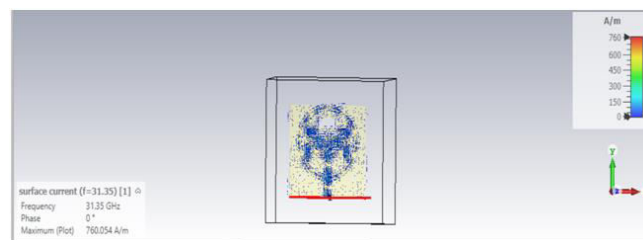


Fig. 13. Surface current distribution at 31.5 GHz

## V. CONCLUSION AND FUTURE SCOPE

The proposed compact CSRR-based antenna design has been successfully analyzed and optimized for operation across multiple mmWave frequencies, specifically at 24.5 GHz, 29.375 GHz, and 31.35 GHz. Simulation results demonstrate efficient impedance matching with return loss values well below -10 dB and VSWR values under 1.5 at the targeted frequencies, confirming the antenna's suitability for high-frequency wireless communication. The far-field radiation patterns reveal highly directional characteristics with sharp main lobes and minimal sidelobe interference, indicating strong performance in focused signal transmission. Additionally, surface current distribution analyses validate the effective radiation behavior of the circular and H-shaped patch structures. This design achieves a balance between compact size, multi-band operation, and good radiation efficiency, making it a promising candidate for 5G and emerging 6G communication systems within the THz band. In future the proposed method can be extended with Physical fabrication of the antenna and experimental validation using vector network analyzers and anechoic chambers will further confirm simulation accuracy. And Exploring alternative substrates with lower loss tangents could further enhance efficiency, especially at higher THz frequencies

## REFERENCES

1. Z. Ren, Y. Chang, Y. Ma, K. Shih, B. Dong, and C. Lee, "Leveraging of MEMS Technologies for Optical Metamaterials Applications," *Fractal Analysis — Applications in Physics, Engineering and Technology*, vol. 8, no. 3, pp. 1900653-190066, 2020.
2. A. Iqbal, B. Abdul, S. Amor, M. Nazih, I. Elfergani, and R. Jonathan, "Electromagnetic Bandgap Backed Millimeter-Wave MIMO Antenna for Wearable Applications," *IEEE Access*, vol. 7, pp. 111135-111144, 2019.
3. W. Lin, R. Ziolkowski, and B. Thomas, "28 GHz Compact Omnidirectional Circularly Polarized Antenna for Device-to-Device Communications in the Future 5G Systems," *IEEE Transactions on Antennas and Propagation*, vol. 65, no. 12, pp. 6904-6914, 2017.
4. U. Ullah, M. Al-Hasan, K. Slawomir, and I. Mabrouk, "Series-Slot-Fed Circularly Polarized Multiple-Input-Multiple-Output Antenna Array Enabling Circular Polarization Diversity for 5G 28 GHz Indoor Applications," *IEEE Transactions on Antennas and Propagation*, vol. 69, no. 9, pp. 5607-5616, 2021.
5. M. Usman, K. Enis, J. Nasir, Z. Yuanwei, Y. Chao, and A. Zhu, "Compact SIW Fed Dual-Port Single Element Annular Slot MIMO Antenna for 5G mmWave Applications," *IEEE Access*, vol. 9, pp. 91995-92002, 2021.
6. M. Usman, K. Enis, J. Nasir, Z. Yuanwei, Y. Chao, and A. Zhu, "A MIMO Dielectric Resonator Antenna with Improved Isolation for 5G mm-Wave Applications," *IEEE Access*, vol. 9, pp. 91995-92002, 2021.
7. M. Sharawi, S. Podilchak, M. Hussain, T. Mohamed, and A. Yahia, "Dielectric Resonator Based MIMO Antenna System Enabling Millimetre-Wave Mobile Devices," *IET Microwaves, Antennas & Propagation*, vol. 11, no. 2, pp. 287-293, 2017.

8. H. Alhaqbani, M. Bait-Suwailam, A. Aldhaeabi, and S. Almoneef, "Wideband Diversity MIMO Antenna Design with Hexagonal Slots for 5G Smart Mobile Terminals," *Progress In Electromagnetics Research C*, vol. 120, pp. 105-117, 2022.
9. M. Bait-Suwailam, S. Almoneef, and S. Saeed, "Wideband MIMO Antenna with Compact Decoupling Structure for 5G Wireless Communication Applications," *Progress In Electromagnetics Research C*, vol. 120, pp. 117-125, 2021.
10. Z. Liu, P. Wang, and Z. Zeng, "Enhancement of the Gain for Microstrip Antennas Using Negative Permeability Metamaterial," *IEEE Antennas and Wireless Propagation Letters*, vol. 12, pp. 429-432, 2013.
11. Z. Pi and F. Khan, "An Introduction to Millimeter-Wave Mobile Broadband Systems," *IEEE Communications Magazine*, vol. 49, no. 6, pp. 101-107, 2011.
12. H. Xu, X. Wang, and Y. Zhang, "Millimeter-Wave Antenna Design for 5G Applications," *IEEE Transactions on Antennas and Propagation*, vol. 67, no. 8, pp. 5123-5132, 2019.
13. S. Park and H. Lee, "Beamforming Techniques for Millimeter-Wave Antennas in 5G Communication," *IEEE Wireless Communications*, vol. 25, no. 5, pp. 85-91, 2018.
14. N. Yadav, R. Prasad, and M. Kumar, "Optimization of 5G Antenna Performance Using Artificial Intelligence," *Sensors*, vol. 23, no. 7, pp. 1278, 2023.
15. X. Zhang and Y. Huang, "Metamaterial-Inspired Antennas for Wireless Communications," *IEEE Antennas and Propagation Magazine*, vol. 59, no. 4, pp. 22-32, 2017.
16. J. Lee et al., "Compact High-Gain Antenna Design for 5G Small Cells," *IEEE Transactions on Antennas and Propagation*, vol. 64, no. 10, pp. 4276-4286, 2016.
17. H. Wang, K. Kim, and J. Park, "A Novel Millimeter-Wave MIMO Antenna for 5G Applications," *IEEE Transactions on Antennas and Propagation*, vol. 68, no. 7, pp. 4821-4830, 2020.
18. Talari, S., & Sekhar, P. C. (2024). A High Gain Dual Band Hexagonal Metamaterial Inspired Antenna for 5G Applications. *Engineering, Technology & Applied Science Research*, 14(6), 18029-18035.



INTERNATIONAL  
STANDARD  
SERIAL  
NUMBER  
INDIA



# INTERNATIONAL JOURNAL OF INNOVATIVE RESEARCH

IN SCIENCE | ENGINEERING | TECHNOLOGY

 9940 572 462  6381 907 438  [ijirset@gmail.com](mailto:ijirset@gmail.com)



[www.ijirset.com](http://www.ijirset.com)

Scan to save the contact details